Materials Chemistry and Physics 312 (2024) 128657

Contents lists available at ScienceDirect

Materials Chemistry and Physics

journal homepage: www.elsevier.com/locate/matchemphys

Activated carbon functionalized with amine sites as an efficient alternative for gold thiosulfate recovery

Nathalie de la Torre-Miranda [a], Pierre Eloy [a], Ernesto de la Torre [b], Timothy Steenhaut [a], Claude Poleunis [a], Sophie Hermans [a,*]

[a] Université catholique de Louvain (UCLouvain), Institut de la Matière Condensée et des Nanosciences (IMCN), Place Louis Pasteur 1, 1348, Louvain-la-Neuve, Belgium
[b] Escuela Politécnica Nacional, Departamento de Metalurgia Extractiva (DEMEX), Ladrón de Guevara E11-253, 17-01-2759, Quito, Ecuador

HIGHLIGHTS

- Active carbon is functionalized with primary and quaternary amine sites.
- The functionalized carbons recover up to 100 % of Au thiosulfate in 2 h contact.
- At acid conditions, an ion-exchange adsorption mechanism has been proven.
- At basic pH, Au^0 species are evidenced in addition to ion-exchange phenomena.
- Au stripping is accomplished with aqueous-based eluents in up to 76 % efficiency.

GRAPHICAL ABSTRACT

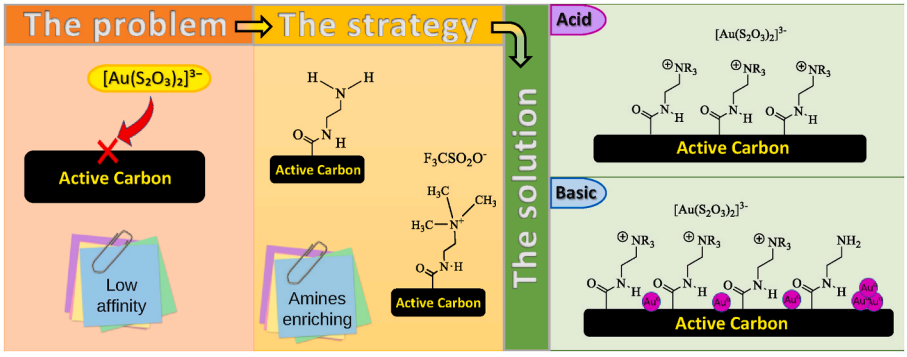

ARTICLE INFO

Keywords:
Active carbon functionalization
Adsorption mechanisms
Amine functions
Gold thiosulfate

ABSTRACT

Thiosulfate is a non-toxic and efficient leaching agent that could be employed instead of cyanide for extracting gold from ores. Nevertheless, it is not commonly used in the gold mining industry due to the challenge that represents the recovery of the formed gold thiosulfate complex from the leachate. Several alternatives such as precipitation methods and adsorption onto amine-rich resins have been attempted for solving this problem. However, neither of them have been proven fully effective or compatible with current hydrometallurgical processes. In this research, the functionalization of granular active carbon with covalently grafted primary and quaternary amine sites is proposed, for enhancing its ability at trapping Au thiosulfate. The functionalized carbons accomplish up to 100 % Au recovery (pristine carbon recovers < 18 % Au) in 2 h (with quaternary aminated carbon), while also being able to operate under acid (pH 4) and basic (pH 9) adsorption conditions. Moreover, ASTM hardness tests estimate that these carbons conserve the mechanical properties needed for being employed in Carbon-in-pulp processes (H > 86%). In-depth solid characterization techniques (XPS, TOF-SIMS, FTIR, PXRD) have revealed that the adsorption mechanism of Au thiosulfate onto amine groups depends on the pH of the solution: at acid pH, an ion exchange mechanism seems to be the dominant process. Under basic conditions, the formation of Au^0 species is evidenced, in addition to ion-exchange phenomena. Elution of the gold loaded samples has been achieved with a yield up to 76 % with $Na_2S_2O_3$ and NaCl solutions.

* Corresponding author.
E-mail address: sophie.hermans@uclouvain.be (S. Hermans).

https://doi.org/10.1016/j.matchemphys.2023.128657
Received 2 July 2023; Received in revised form 16 October 2023; Accepted 4 November 2023
Available online 8 November 2023

1. Introduction

Cyanidation has been one of the most used gold leaching techniques in several mining facilities around the world since its invention in the 1800s. It is chosen due to its technical simplicity, efficiency and low cost, despite its high environmental impact and toxicity [1,2]. This process consists in contacting the previously ground ore with a cyanide salt solution (commonly NaCN or KCN), which will leach gold from the auriferous ore by forming the stable Au cyanide complex. Then, typically, AuCN is recovered from the pregnant solution by either precipitation methods through the addition of Zn powders (Merrill-Crow) [3] or by adsorption on active carbons (Carbon-in-Pulp) [4].

Nowadays, however, sustainable development policies implemented in several countries are pressing to reduce or ban the use of toxic compounds like cyanide in gold extraction activities, being therefore imperative to propose sustainable alternatives. In this context, thiosulfate is seen as an appropriate choice since it is both, a non-toxic and highly efficient leaching agent, even when employed with carbonaceous or complex ores, where cyanide shows lower performances [1,2,5].

Thiosulfate ($S_2O_3^{2-}$) is a metastable sulfur compound with a strong capacity for metal (e.g. Au, Ag, Cu, Fe, Ni, Co) complexation. It achieves to dissolve gold from auriferous ores in alkaline conditions (typical working pH: 9–11), in the presence of an oxidant like oxygen, forming the stable, anionic complex $[Au(S_2O_3)_2]^{3-}$. Usually, to increase the gold dissolution rate, leaching is carried out in the presence of ammonia and copper ions. By a close control of leaching conditions (e.g. concentration of species, pH), Au dissolution is usually effective. However, in the practice, the use of thiosulfate in the gold mining industry is scarce due to the fact that recovering $[Au(S_2O_3)_2]^{3-}$ from the leachate is challenging. Several alternatives have been proposed for solving this problem including: precipitation methods with Zn, Al or Cu powders; solvent extraction techniques with esters or amines in organic media; direct adsorption onto active carbons or basic polymeric resins with amine sites. However, neither of them have been, up to date, proven effective due to numerous application drawbacks. For instance, precipitation methods may involve high costs due to elevated consumption of precipitation agents and complex after-process product purifications. Regarding solvent extractions methods, the use of organic solvents is required for gold recovery in organic medium, which is incompatible with installed on-site hydrometallurgical facilities. Additionally, the separation of Au and other metals in these conditions is sometimes too complex and obtaining a high purity product is problematic. Concerning active carbon, even though this is the main sorbent chosen for AuCN recovery, in thiosulfate systems, it shows poor performances, due to its lack of affinity for the $[Au(S_2O_3)_2]^{3-}$ complex. Considering resins adsorption, despite possessing high loading capacities and good affinity for Au thiosulfate, their main drawbacks lay on their brittleness, making it challenging to work directly in contact with mineral pulps that are really abrasive, their small particle sizes (usually some μm) which necessitate fine filters and pricey centrifugation techniques for separation and their sensitivity to osmotic shock. For all these reasons, thiosulfate's applicability to the industry is limited so far to minerals with preg-robbing carbon [1,2,6,7].

Activated carbon (AC) is a type of carbon material employed in a variety of applications in different forms (granular, powdered, extruded, *etc*.), thanks to its high adsorption capacity of organic and inorganic molecules and complexes. For example, granular active carbons are preferred in Carbon-in-Pulp processes for Au cyanide adsorption instead of resins, due to their high mechanical resistance to abrasion, making it possible to work directly in contact with mineral pulps [8]. Additionally, powdered active carbons are daily employed for water and air depollution in homes and factories, as they are cheap and versatile [9].

The adsorption of a specific compound on a given active carbon depends on both its physical structure (active carbons are characterized by a high surface area and well-developed microporosity) and unique chemical composition [10–12]. Indeed, the presence of different heteroatoms on the carbon's surface is the key for its chemical reactivity [12]. These heteroatoms (e.g. oxygen, nitrogen, sulfur, phosphorus, *etc*.) could come from the raw material employed in the carbon's production, or could be intentionally added by specific functionalization procedures, thanks to which, they can be tuned for working in a desired application [13]. For instance, in other research works, carbon materials have been functionalized with basic functions for their employment in polymer and electrochemical applications, sensors development, H_2S adsorption, selective metal removal from aqueous media and biomaterials [14–20].

In the context of gold thiosulfate recovery, grafting nitrogen functional groups (specifically amines sites) represents an attractive functionalization strategy, that may increase the affinity of active carbon for this complex, since it is known [6] that amine sites (primary, secondary, tertiary or quaternary) are the acting agents present in commercial weak and strong base resins used for this purpose. Indeed, amine groups can be protonated when immersed in aqueous solutions [21] and, thanks to this property, they could electrostatically attract anionic compounds like $[Au(S_2O_3)_2]^{3-}$ [7]. By producing an amine-functionalized carbon, we could obtain the best characteristics of both solids: amines as trapping group for gold thiosulfate, grafted onto resistant granular active carbon, which is compatible with Carbon-in-Pulp processes. As far as we know, no published work has covalently functionalized granular active carbon with amine groups for gold thiosulfate recovery. The only similar approaches found in the literature are the research of Fotoohi and Mercier [7], who have functionalized mesoporous silica with primary amine sites and Zhao Li et al. [22], who have worked on the functionalization of chloromethylated polystyrene with quaternary amines. However, since silica and chloromethylated polystyrene have small particle sizes [6], they may face similar problems as resins, due to the difficulty in separating the gold-loaded silica from the mineral pulp by simple filtration methods. Furthermore, the interaction mechanism between gold (I) thiosulfate and amine groups covalently anchored on activated carbon has not been studied, as far as we know, neither the influence of pH in Au adsorption. Since the protonation and deprotonation of amine sites (and therefore, their Au adsorption capacity) might strongly depend on the solution pH, a deeper study of the adsorption mechanism under acid and basic conditions would be relevant to accomplish a complete understanding of the phenomena. Furthermore, no research has been found concerning the evaluation of elution strategies of the gold loaded aminated carbons by green aqueous eluents.

Hence, the goal of this research is to develop a covalently primary or quaternary amine functionalized granular active carbon, capable of efficiently trapping $[Au(S_2O_3)_2]^{3-}$. The idea is to create a new solid enriched with primary or quaternary amine sites, which would augment its adsorption performance, while conserving its mechanical properties, allowing its potential use in industrial Carbon-in-pulp processes. Therefore, the chemical functionalization process will be carried out directly on active carbon grains and not on carbon powders, to remain in alignment with its actual application in the gold mining industry.

The functionalization method that will be implemented has been previously used in other researches for metal nanoparticles anchoring [23–25]. It involves the oxidation of the material with a strong oxidant for enriching the surface with carboxylic acid groups, followed by an acylation step that will facilitate the grafting of the desired amine through the formation of an amide bond. For primary amine functionalization, ethylenediamine is added to obtain an $–NH_2$ terminal. If quaternary amine functionalization is desired, the peptide bond is formed with a tertiary amine and then a quaternization reaction is carried out with a methylating agent for obtaining the required functional group. Fig. 1 shows schematically both functionalization pathways.

After functionalization, the amine-grafted carbon grains will be tested with Au thiosulfate solutions to explore their gold adsorption kinetics and their adsorption performances at different gold concentrations and pHs (acid and basic). Moreover, some elution strategies with green, aqueous-based eluents will be tested for gold stripping.

Furthermore, the functionalized carbons will be verified with an ASTM Hardness Test method to assess their mechanical resistance to abrasion and value its compatibility with Carbon-in-Pulp processes. Finally, the mechanism of gold thiosulfate interactions with the different amine sites under basic and acid adsorption conditions will be investigated by in-depth characterization techniques, bringing new fundamental knowledge.

2. Experimental

2.1. Materials and reagents

All functionalization experiments were carried out on a granular, coconut shell-based commercial active carbon (Calgon Carbon GRC 20/22), which is commonly employed in Carbon-in-Pulp processes for AuCN adsorption. Average particle size: 2.5 ± 0.9 mm (mesh 6 x 14). The following reagents were used as received: nitric acid (HNO_3, 65 %, Roth), thionyl chloride ($SOCl_2$, 99.7 %, Acros Organics), sodium hydroxide (NaOH, 99.2 %, VWR), toluene ($C_6H_5CH_3$, 100 %, VWR), N,N-dimethylethylenediamine ($C_4H_{12}N_2$, 95 %, Merk), ethylenediamine ($C_2H_8N_2$, ≥99 %, Sigma Aldrich), methyl trifluoromethanesulfonate ($CF_3SO_3CH_3$, ≥97 %, Alfa Aesar), Argon (α1, Air liquide), gold (I) sodium thiosulfate hydrate ($Na_3Au(S_2O_3)_2 \bullet xH_2O$, 99.9 %, Alfa Aesar), ammonium hydroxide solution (28.8 % NH_3 basis, Sigma Aldrich), sodium thiosulfate anhydrous ($Na_2S_2O_3$, 99 %, Alfa Aesar), sodium chloride (NaCl, 99 % Sigma-Aldrich), sodium sulfite (Na_2SO_3, 98 %, Acros Organics), sodium hydroxide standard solution (NaOH, 1 mol/L, Merk), sodium carbonate standard solution (Na_2CO_3, 0.05 mol/L, Merk), sodium bicarbonate ($NaHCO_3$, ≥99.7 %, Sigma Aldrich), hydrochloric acid (HCl, 37 %, VWR), potassium bromide (KBr, for spectrometric IR use, Roth), pH buffer solutions (pH 4, 7, 10, Alfa Aesar, ±0.01), gold standard solution for atomic absorption (999 mg/L ± 4 mg/L, Sigma Aldrich), deionized water, technical-grade acetone (Lambert Chemicals).

2.2. Characterization methods and techniques

The functional groups in active carbons were characterized using Fourier transform infrared spectroscopy (FTIR) in transmission mode (Bruker Alpha spectrometer with DTGS detector). To reduce the interference of water and carbon dioxide in the spectra, the apparatus was located inside a globe box with argon atmosphere. The spectra were collected in the range 600–4000 cm^{-1} (resolution: 2 cm^{-1}) with 100 scans. The analysis was carried out on KBr – active carbon pellets (dilution rate: 0.5 wt% AC). The pellets were prepared by combining together active carbon and KBr and milling the mixture until the particle size was less than 100 μm. Then, the KBr-carbon mixture was pressed (10 tons) to form the pellet, which was dried under vacuum overnight before analysis. The OPUS software version 7.5 was used to exploit all the spectra.

The concentration of gold in solution was determined by Atomic Absorption Spectrometry (AAS). The analysis was carried out with a PerkinElmer 3110 instrument. Several calibration curves in the range of 2–25 ppm were performed by diluting a commercial gold standard solution.

X-ray photoelectron spectroscopy (XPS) was employed for chemical surface characterization of modified active carbons. For this purpose, a SSX 100/206 photoelectron spectrometer (Surface Science Instruments, USA) equipped with a monochromatized micro focused Al X-ray source (powered at 20 mA and 10 kV) was used. The analyses were done directly on active carbon grains (approximate analyzed area: 1.4 mm^2) by fixating them with double-sided tape onto small brass troughs (Ø 6 mm), that were placed on a ceramic carousel. The pressure in the analysis chamber was ≈10^{-6} Pa, the angle between the surface normal and the axis of the analyser lens was 55°, and the pass energy was 150 eV. The flood gun was set at 8 eV and a Ni grid placed 4 mm above the samples was employed for charge stabilisation. Under these conditions, the full width measured at half maximum (FWHM) of the Au $4f_{7/2}$ peak for a clean gold standard sample was ≈1.6 eV. The following sequence of spectra was recorded: survey scan, C 1s, O 1s, N 1s, Au 4f $_{7/2}$, and C 1s again, to check charge stability compensation in time. The spectra were calibrated using the C 1s peak, fixing the position of C- (C,H) component at ≈284.6 eV. Data treatment was done with CasaXPS program (Casa Software Ltd, UK) where the spectra were decomposed with the least squares fitting routine with a Gaussian/Lorentzian (85/15) product function subtracting a Shirley baseline. Molar fractions were calculated using peak areas normalized based on acquisition parameters and sensitivity factors provided by the manufacturer.

ToF-SIMS (Time of Flight Secondary Ion Mass Spectrometry) was also employed for surface characterization of modified active carbons. The analysis was done in a TOF.SIMS5 instrument (IONTOF GmbH, Münster, Germany). A primary beam was produced by a pulsed Bi^{3+} metal ion source using an acceleration voltage of 30 kV. An AC target current of 0.3 pA with a bunched pulse width lower than 1 ns was applied. The analysis was done in both positive and negative mode. For spectra acquisition, a raster of 128 x 128 data points over an area of 200 × 200 μm^2 was employed. The total primary ion beam dose for each analyzed area was always kept below 5 $x10^{11}$ ions.cm^{-2}, for static conditions maintenance. A lateral resolution of ~3 μm and mass resolution $m/\Delta m > 5500$ at 49 *m/z* were maintained for positive and negative

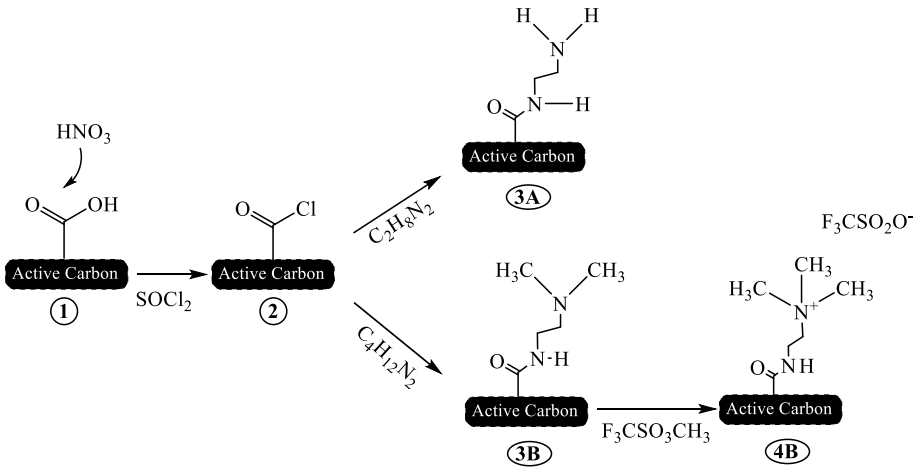

Fig. 1. Primary and quaternary amine functionalization processes: 1) Oxidation (giving solid named ACox), 2) Acylation. 3A) Primary amine formation (giving functionalized AC-NH_2), 3B) Peptide bond creation with tertiary amine. 4B) Quaternary amine formation (giving AC-NMe_3^+).

spectra acquisition. No charge compensation was necessary. The obtained spectra were analyzed with the software SurfaceLab (version 6.5), supplied by the manufacturer. Active carbon grains were sticked onto Ag conductive double side adhesives and introduced directly in the instrument chamber for being analyzed.

Powdered X-ray diffraction (PXRD) was used for analyzing ground active carbon samples (particle size <100 μm). The analysis was performed with an Incoatec Microfocus Source^{HIGHBRILLIANCE} (IμS^{HIGHBRILLIANCE}) Mo ELM47 source (MAR345 image plate detector) operating at 50 kV and 1000 μA, at a wavelength of 0.71073 A° (Mo K α radiation). The samples were filled in glass capillaries (0.7 mm diameter) and were exposed to X-rays for 15 min, while the capillary was rotated by 180°. Fit2D software was used for data integration (using data from a 0.1 mm diameter capillary filled with LaB_6 as calibrant).

The pH of solutions was determined with a pH-meter (Eutech Instruments pH510 equipped with a SI Analytics N54 BNC probe), which was calibrated before analysis with 4, 7 and 10 pH buffer commercial solutions.

The Point of Zero Charge (PZC) of active carbons was determined through the Park and Regalbuto methodology [26]. In a typical experiment, 1 g of AC was placed in a 25 mL Erlenmeyer along with 10 mL of deionized water, whose pH was previously measured and regulated at a determined pH value by adding either HCl or NaOH. Then, the carbon was agitated for 24 h, after which the solution's pH was measured again, to determine the final pH after contact. This procedure was repeated over a wide range of initial pHs (1.5–13.5) and a graph comparing the variation of initial vs final pH was elaborated to establish the PZC value, which corresponds to the plateau of such curve.

Active carbon's acidity and the presence and nature of oxygen functional groups were determined by Differentiate Boehm titrations. This characterization method is described elsewhere [27–29]. In a typical experiment, 0.5 g of AC grains were put in contact with a basic solution (0.05 M) of either NaOH, Na_2CO_3 or $NaHCO_3$ for 24 h. Afterwards, the carbon was filtrated and an aliquot (10 mL) was taken. Then, HCl solution (0.05 M) was added for acidification (20 ml if NaOH or $NaHCO_3$ were used as base and 30 mL if Na_2CO_3 was employed) and this solution was degassed using Ar (at least 2 h). Lastly, the degassed solution was titrated with degassed NaOH solution (0.05 M) using phenolphthalein as indicator.

Active carbon was tested with the Standard Test Method for Ball-Pan Hardness of granulated active carbons according to norm ASTM D3802-79 (1999) [30], to assess its degree of hardness before and after functionalization processes. In a typical experiment, the material (original particle size: mesh 6 x 14) was put in a hardness pan along with several steel balls (ø 12.7 mm and 9.5 mm). Then, it was shaken in a mechanical sieve-shaker with tapping hammer (ATM Arrow) for 30 min. After this time, the balls were removed and cleaned with a brush and the carbon was transferred to a hardness test sieve (mesh No. 25). The carbon was then sieved for 10 more minutes in the sieve-shaker. Finally, the Ball-pan hardness number (H %) was calculated with Eq. (1), where B is the amount of carbon that was retained on the hardness test sieve and A corresponds to the amount of carbon originally loaded into the hardness pan.

$$H\,\% = 100 * \frac{B}{A} \qquad \text{Eq. (1)}$$

2.3. Methods

2.3.1. Amine covalent functionalization

Active carbon was covalently functionalized with either quaternary or primary amine sites following a procedure described elsewhere [23–25]. For the functionalization with quaternary amines, the following four-step process was performed:

1. **Oxidation**: 4 g of AC were put in contact with 400 mL of HNO_3 (2.5 M) for 6 h. The system was agitated and heated at 105 °C, under reflux, using a NaOH trap for acid vapors. Subsequently, the carbon was filtrated out, washed with plenty of deionized water (at least 2 L) and dried under vacuum for several hours. The oxidized carbon will be referred to hereinafter as ACox.
2. **Acylation:** ACox was acylated with 20 mL of $SOCl_2$ in toluene medium (130 mL) at 120 °C for 5 h, under agitation. After that, the solid was filtrated, washed with 500 ml of toluene and dried overnight under vacuum.
3. **Peptide bond creation with tertiary amine:** The acylated carbon was dispersed in 170 mL of toluene along with 1.3 equivalents of N, N-dimethylethylenediamine, calculated according to the total amount of acidic functions in ACox determined by Boehm Titrations. The dispersion was heated at 120 °C and mixed for 4 h. Then, the carbon was filtrated, washed with 500 ml of toluene and dried under vacuum for several hours.
4. **Quaternary amine formation:** Lastly, the carbon described in step 3 was agitated with $CF_3SO_3CH_3$ (5 equivalents according to estimated acidic functions in ACox) in 200 mL of acetone for 24 h at room temperature (RT). Afterwards, the sample was filtrated, washed with 500 ml of acetone and dried under vacuum for several hours. The so-obtained quaternary amine functionalized carbon will be referred to hereinafter as AC-NMe_3^+.

The functionalization process to obtain primary amine sites involved the carbon's oxidation and acylation (steps 1 and 2) as described above. Afterwards, the acylated carbon was put in contact with ethylenediamine (1.3 equivalents according to ACox total estimated acidic functions) in toluene medium (170 mL) at 120 °C for 4 h. Finally, the carbon was filtrated, washed with 500 ml of toluene and dried under vacuum for several hours. This primary amine functionalized carbon will be referred to hereinafter as AC-NH_2. A scheme illustrating the functionalization process to enrich carbon with quaternary and primary amine sites is shown in Fig. 1.

2.3.2. Gold thiosulfate adsorption tests

Non-functionalized and functionalized active carbons were tested with gold thiosulfate solutions to assess their adsorption capacity. In a typical experiment, 0.5 g of AC were agitated with 100 mL of gold thiosulfate solution at RT for 24 h. Then, the solid was recovered by filtration, dried for several hours and stored before its characterization, while the filtrate was analyzed by AAS to determine the amount of gold in solution. Gold thiosulfate solutions were prepared by dissolving an exact quantity of $Na_3Au(S_2O_3)_2 \bullet xH_2O$ in water until obtaining a desired concentration: 2 mg/L, 10 mg/L or 25 mg/L (Au basis). These solutions were analyzed before use with AAS to assess their exact gold content. The tested concentrations were chosen considering the typical gold contents of real leachates obtained from minerals which are currently exploited with cyanidation and Carbon-in-pulp processes [31–33].

To determine the influence of pH on gold adsorption, some tests were carried out under different pH conditions: at ≈ pH 4, which is the unshifted pH of the gold solution and ≈ pH 9, which is the typical pH found in leachates coming from real auriferous ores processed in Carbon-in-Pulp facilities [2]. The pH was adjusted by adding few drops of NH_4OH. For these experiments, the initial Au thiosulfate solution concentration was always 25 ppm. The gold loaded carbons will be named AC-NH_2.Au and AC-NMe_3^+.Au followed by the pH at which the adsorption was carried out.

Active carbon gold adsorption efficiency (% R) was calculated according to Eq. (2), where Ci (mg/L) is the Au concentration of the solution before active carbon contact, and Cf (mg/L) is the gold concentration after contact:

$$\%\,R = \frac{Ci - Cf}{Ci} * 100 \qquad \text{Eq. (2)}$$

2.3.3. Elution tests

Elution tests consisted in two phases: 1) Gold loading phase: carried out according to the procedure described above at point 2.3.2 (Initial Au concentration in solution: 25 ppm, pH 4 or pH 9). 2) Elution phase: The gold loaded carbons were agitated with 25 mL of a selected eluent for 24 h at 50 °C. For heating, an oil bath was used along with a cold-water refrigerant to minimize evaporations. When the contact time had passed, the carbon was filtrated while the solution was transferred to a 50 ml volumetric flask. The eluted AC was washed with water and the washings added directly to the flask until reaching its graduation mark. This solution was analyzed by AAS for calculating the mass of gold in the eluent. The eluted carbon was dried and stored before its characterization. The elution efficiency was determined with Eq. (3), by comparing the mass of Au in the eluent and the mass of Au in the carbon before elution.

$$\%\ elution\ efficiency = \frac{mass\ of\ Au\ in\ eluent}{mass\ of\ Au\ in\ AC\ before\ elution} * 100 \qquad \text{Eq. (3)}$$

Elution solutions were prepared by dissolving an exact amount of reagent in water to obtain a desired molar concentration (M). Two elution solutions were tested: NaCl (2 M) + Na_2SO_3 (0.1 M) and $Na_2S_2O_3$ (1 M) + NH_4OH (0.1 M).

3. Results and discussion

3.1. Active carbon oxidation

The presence of heteroatoms on the surface of active carbon (AC) confers it specific characteristics, properties and reactivity towards certain molecules [10,34]. These heteroatoms may remain from the raw materials used in their production or could be incorporated post-synthetically in the carbon matrix by different chemical functionalization methods [10,11]. For instance, active carbon can be oxidized by liquid oxidants like HNO_3, which will increase its acidity due to the creation of new oxygen groups on its surface such as carboxylic acids, lactones and phenols [27,35,36]. These groups, and especially carboxylic acids, can be used as "anchor functions" to graft other functionalities of interest [23,37], which may have good affinity towards gold complexes within the present context. Hence, a granular active carbon used commercially for Carbon-in-Pulp processes was treated with nitric acid to increase the number of carboxylic acid groups on its surface.

To assess the presence of new oxidized species after HNO_3 treatment, ACox was characterized by Differentiate Boehm Titrations, XPS and FTIR. As shown in Fig. 2, Boehm titrations evidence a notable augmentation of the carbon's total acidity after oxidation, from 8 mmol/100 g AC (Blank) to 156 mmol acid sites/100 g AC (ACox). Differentiate Boehm Titrations allow to determine and quantify the type of oxygen groups present in the solid: the main acid functionality found in ACox is carboxylic acid groups (80 mmol/100 g AC), followed by phenols (43 mmol/100 g AC) and lactones and (33 mmol/100 g).

XPS analysis corroborates the oxidation of carbon after HNO_3 treatment. As shown in Table 1, the total atomic oxygen surface content (Total O) of ACox increased from 8.6 at.% (Blank) to 15.8 at. %. The same tendency is seen when comparing the amount of O linked to C with the total C detected in the sample (O–C/Total C), which is augmented from 0.09 to 0.23, evidencing that the increase in atomic oxygen detected on ACox actually comes from oxidized species linked to the carbon matrix. Moreover, these results are in accordance with the increase of acidity measured by Boehm Titrations, which demonstrates that a more acidic sample contains more oxygen on its surface. Similar observations were done by S. Hermans et al. [38], who demonstrated a linear correlation between the sample's total acidity measured by Boehm Titrations and the O/C ratio detected by XPS.

Finally, FTIR analysis corroborates the presence of different oxygen groups in ACox, that were not detected on Blank. As illustrated in Fig. 3,

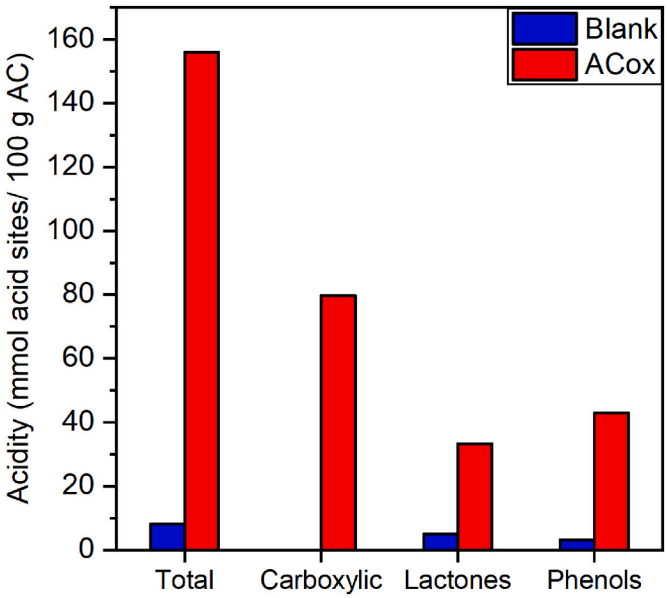

Fig. 2. Differentiate Boehm titrations of non-oxidized (Blank) and HNO_3 oxidized active carbon (ACox).

Table 1
Comparison between Boehm titrations and XPS analysis of non-oxidized (Blank) and oxidized active carbon (ACox).

Sample	XPS analysis		Total acidity (mmol/100 g AC)
	Total O (% at.)	O–C/Total C	
Blank	8.6	0.09	8
ACox	15.8	0.23	156

ACox spectrum shows a band at ≈ 1720 cm^{-1}, corresponding to the C═O stretching of carbonyl groups coming from carboxylic acids, lactones or ketones [35,39,40] and a band at ≈ 1570 cm^{-1} that could be assigned to highly conjugated C═O groups [35] or C═C aromatic ring stretching vibration [39]. Additionally, it could be noticed that the intensity of a broad band at ≈ 1100 cm^{-1} in ACox is increased compared to the Blank. This could be due to the presence of alcoholic C–O stretching of phenols and O–H bend/stretching [39,40]. Lastly, a sharp band at ≈ 1384 cm^{-1} attributed to NO_3 asymmetric stretching and another found at ≈ 810 cm^{-1}, assigned to NO bending vibration [40] denote the presence of inorganic nitrates. These nitrates could come from HNO_3 residue in the sample.

3.2. Amination

The presence of amine groups on the surface of the functionalized carbons by the two envisaged pathways (AC-NH_2 and AC-NMe_3^+, see Fig. 1) was confirmed by XPS, TOF-SIMS and FTIR analysis. Firstly, the XPS N 1s high resolution (HR) spectra of Blank (Fig. 4 A) evidences a peak located ≈406.7 eV, which could be attributed to an oxidized form of nitrogen like nitrates (C–NO_3) [41]. This species is the main component (Area 56 %) as well in the carbon after oxidation with HNO_3 (ACox), as it could be observed in Fig. 4 B. In contrast, after functionalization with primary amines, the N 1s HR peak of AC-NH_2 shows new nitrogen species located at lower binding energies (Fig. 4C). This peak was resolved in four components positioned at ≈ 398.7 eV, 399.9 eV, 401.5 eV and 403.8 eV. The first one located at ≈398.7 eV could be attributed to aromatic nitrogen inside the carbon matrix (e.g. pyridines) [42,43]. The peak at ≈ 399.9 eV, which is the most significant component (49 % of the peak's area), denotes the presence of amine groups or amides (due to the amide coupling expected in the reaction) [23,42,44].

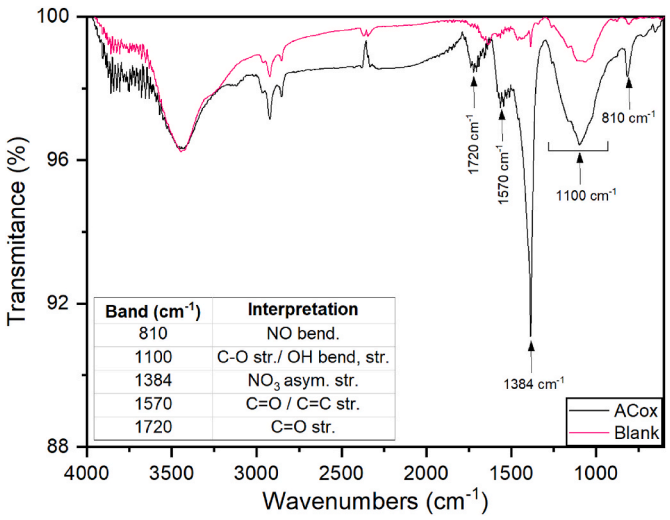

Fig. 3. FTIR spectra of non-functionalized (Blank, pink line) and HNO_3 oxidized active carbon (ACox, black line). (For interpretation of the references to colour in this figure legend, the reader is referred to the Web version of this article.)

This corroborates the success of the covalent functionalization process, since both an $–NH_2$ terminal and the amide bond are expected in this sample. The component at ≈ 401.5 eV indicates a possible protonation of the nitrogen involved in the amide coupling/amine terminal due to the analysis conditions [43,45]. Lastly, the small peak (Area: 7%) at ≈ 403.8 eV could be assigned either to nitrites [46], or to the presence of a shake-up, which could appear because of the aromatic character of the carbon matrix, where the nitrogen species are grafted.

TOF-SIMS analysis confirms the information obtained by XPS. Fig. S1 shows the most relevant fragments detected in the positive ion spectrum of AC-NH_2. First, at $m/z \approx 17.03$, the fragment $–NH_3^+$ is detected in the positive mode, attributed to the protonated primary amine. Moreover, at $m/z \approx 87.08$, the complete fragment $CO–NH–CH_2-CH_2-NH_2^+$ is evidenced, confirming the amide coupling and the presence of the expected functional group that is covalently bounded to the carbon matrix.

In FTIR analysis, several new bands that reveal the existence of amines are detected in the functionalized carbon. Fig. 5 shows the FTIR spectra of AC-NH_2, where the following main bands are observed: a broad band centered at ≈ 3150 cm^{-1}, corresponding to N–H stretching of amine or amides [40,47], a band centered at ≈1550 cm^{-1}, characteristic of N–H bending vibration [7,47] or N–H deformation of primary amines [48], a band at ≈ 1200 cm^{-1} corresponding to C–N stretching vibration [40,49] and a sharp band at 1384 cm^{-1} assigned to NO_3 asymmetric stretching [40].

Regarding AC- NMe_3^+, the N 1s XPS HR peak (Fig. 4 D) evidences as well the presence of new nitrogen species created due to the functionalization process, for obtaining quaternary amine sites. Similar to AC-NH_2, the N 1s HR peak of AC-NMe_3^+ was resolved in four components located at: ≈398.5 eV, 399.6 eV, 401.6 eV and 404.5 eV. The interpretation of these species is similar to AC-NH_2, described above: at ≈ 398.5 eV, aromatic nitrogen inside the carbon matrix; at ≈ 399.6 eV, amine or amide groups; at ≈ 404.5 eV, nitrites or shake-up [23,24,42,44,46].

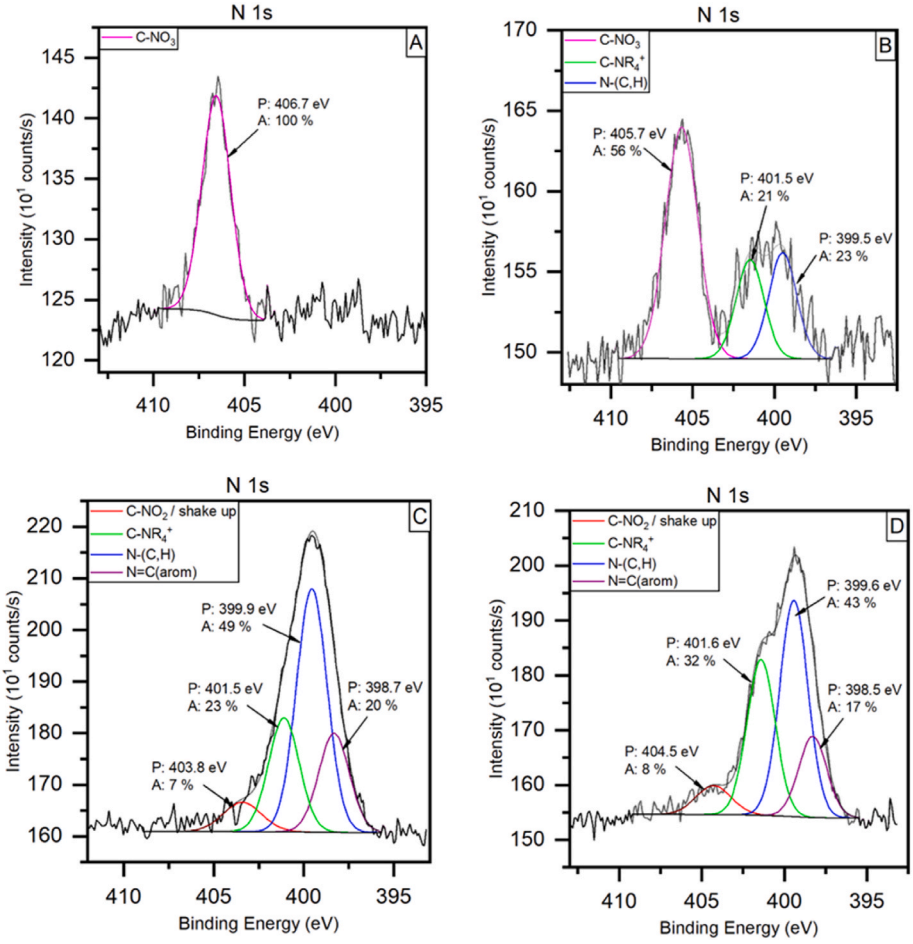

Fig. 4. N 1s XPS HR peak of: A) Blank, B) ACox C) AC-NH_2, D) AC-NMe_3^+. In the graphs, P: Position of the component (eV), A: area percentage that represents the component % contribution inside the whole peak envelope.

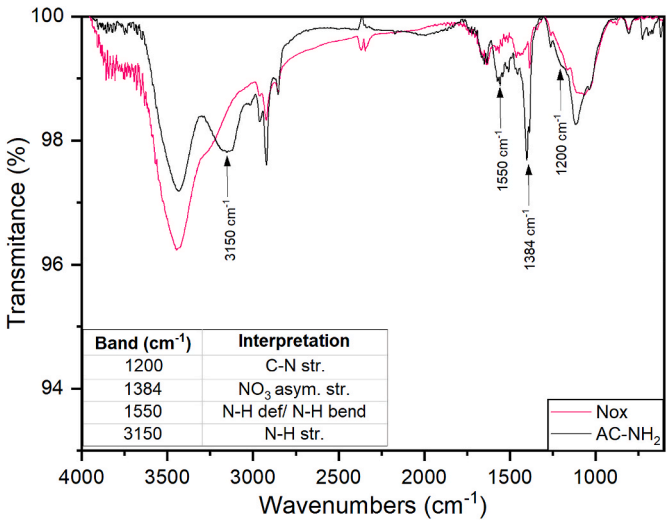

Fig. 5. FTIR spectra of non-functionalized (Blank, pink line) and primary aminated (AC-NH_2, black line) active carbons. (For interpretation of the references to colour in this figure legend, the reader is referred to the Web version of this article.)

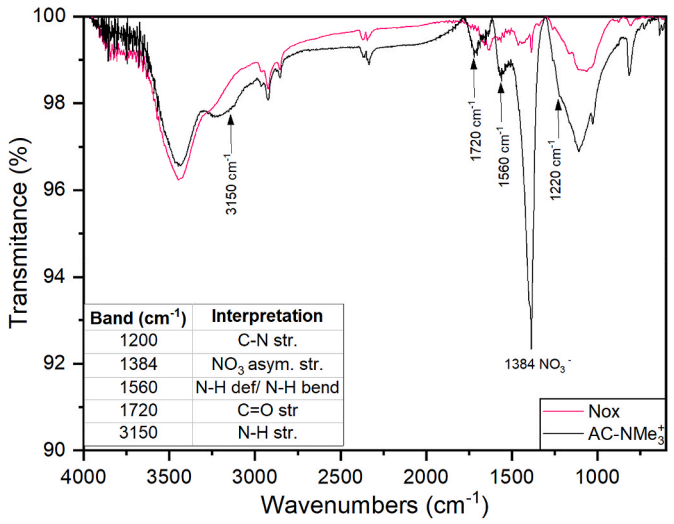

Fig. 6. FTIR spectra of non-functionalized (Blank, pink line) and quaternary aminated (AC-NMe_3^+, black line) active carbons. (For interpretation of the references to colour in this figure legend, the reader is referred to the Web version of this article.)

Lastly, the component at ≈ 401.6 eV is attributed to protonated nitrogen species [23,24,42]. It is important to notice that the size of this peak (Area: 32 %) is considerably bigger than the one detected in AC-NH_2 (Area: 23 %), which indicates that the amount of charged nitrogen in this sample is more important and therefore, that the -NMe_3^+ terminal is present.

AC-NMe_3^+ TOF-SIMS analysis corroborates XPS results. Fig. S 1 shows the most relevant fragments detected in the positive and negative ion spectra of this sample: at $m/z \approx 72.09$, the fragment HC-N-$(CH_3)_3^+$ is evidenced in the positive mode, confirming the expected functional group. Moreover, the counter-ion $F_3C^{34}SO_2O^-$ appears at $m/z \approx 150.96$, in the negative mode, which verifies the existence of this anion in the solid.

Regarding AC-NMe_3^+, FTIR spectrum (Fig. 6), the following main bands are noted: a broad band centered at 3150 cm^{-1}, corresponding to N–H stretching of amine/amides [40]; a band at 1720 cm^{-1}, attributed to the C═O stretching of oxidized carbon species [40], which may be present due to the sample's prior oxidation; a band at 1560 cm^{-1} assigned to N–H bending vibration [50,51], a sharp band at 1384 cm^{-1} attributed to NO_3 asymmetric stretching [40] and a band at 1220 cm^{-1} assigned to C–N stretching [49].

Finally, the total nitrogen surface content (at. %, excluding H) quantified by XPS in both functionalized samples (AC-NH_2: 5.1 at. %; AC-NMe_3^+: 3.9 at. %) is more important than the amount of N detected in the Blank (0.8 at. %) and in ACox (1.4 %), as could be compared in Table 2. This means that the functionalization process has increased the N content in the treated carbons, as expected, and reconfirms the carbon's amination.

3.3. Hardness tests

The functionalization procedures that were carried out to enrich AC grains with primary and quaternary amine sites could have had an impact on the carbon's structure. For instance, it is known that HNO_3 oxidation could modify the active carbon's porous structure, cause pore blockage and even cause carbon's degradation to humin substances [52]. These changes could compromise its mechanical resistance to abrasion, which is a determinant factor for its application in gold-mining processes, since brittle and fine carbon means more gold losses [53]. The Ball Pan Hardness test is a common industrially used method to estimate the resistance of granular active carbons during Carbon-in-Pulp processes and it will permit the comparison of samples before and after functionalization. The hardness tests results are shown in Table 3. As it could be observed, while the Ball Pan Hardness number (H) of Blank is 95.1 %, the primary and quaternary aminated samples present 88.7 % and 86.8 %, respectively. This confirms that the functionalization processes do have an impact on the carbon's mechanical resistance. However, their H values are still inside the acceptable range for granular active carbons employed in mining applications, whose H value could vary from 82.8 to 99 % [54]. Therefore, these functionalized carbons could be applied in gold extracting practices without further processing like pelletization. This is a key characteristic that put the functionalized carbon competitively ahead of amine-rich resins, since it is hard enough to be employed in Carbon in Pulp processes.

Table 2
XPS analysis of non-functionalized, oxidized, aminated and gold-loaded samples: Total nitrogen surface content quantification (% at. excluding H) and N 1s components attributions with their positions.

Sample	Total N content (% at.)	N 1s components				
		C–NO_2 or shake-up	C–NO_3	C-NR_4^+	N-(C, H)	N═C (arom)
		XPS peak's position (eV)				
Blank	0.8 ± 0.5	–	406.7	–	–	–
ACox	1.4 ± 0.3	–	405.7	401.5	399.5	–
AC-NH_2	5.1 ± 0.5	403.8	–	401.5	399.9	398.7
AC-NMe_3^+	3.9 ± 0.9	404.5	–	401.6	399.6	398.5
AC-NH_2. Au pH4	5.3 ± 0.6	403.8	–	401.7	400.1	398.9
AC-NMe_3^+. Au pH4	3.3 ± 0.2	405.2	–	402.0	400.1	398.8
AC-NH_2. Au pH9	5.1 ± 0.4	403.6	–	401.4	399.9	398.7
AC-NMe_3^+. Au pH9	4.2 ± 0.5	404.2	–	401.9	399.9	398.9

Note: The Standard deviations shown in this table have been calculated between samples of the same type, synthetized and analyzed at different moments.

Table 3
Hardness tests according to the norm ASTM D3802-79 (1999) of non-functionalized (Blank) and functionalized (AC-NH_2, AC-NMe_3^+) active carbons.

Sample	H (%)
Blank	95.1 ± 0.7
AC-NH_2	88.7 ± 0.5
AC-NMe_3^+	86.8 ± 0.8

3.4. Gold adsorption tests: influence of Au solution concentration and kinetics

Fig. 7 illustrates the gold recovery performances of the non-functionalized (Blank) and aminated (AC-NH_2, AC-NMe_3^+) samples, at different initial gold concentrations (all these Au adsorptions were done at pH 4). Under these conditions, it is evident that the presence of amine sites, either primary or quaternary amines, on the carbon's surface enhances its ability to adsorb $[Au(S_2O_3)_2]^{3-}$, accomplishing a gold uptake of up to 100 % at 2 and 10 ppm gold initial concentrations, compared to notably lower recovery performances of the non-functionalized one. Then, when the initial gold concentration is 25 ppm, this efficiency enhancement is more remarkable. While AC-NH_2 and AC-NMe_3^+ achieve a gold adsorption performance of ≈95 % and ≈96 %, respectively, the Blank's efficiency is just 8 %.

Furthermore, by analyzing the kinetics data (% gold recovery in function of time) shown in Fig. 8, it can be noticed that AC-NMe_3^+ shows a high efficiency, getting a complete gold recovery in just 2 h contact. This may mean that $[Au(S_2O_3)_2]^{3-}$ has a strong affinity for the quaternary amine sites that were grafted onto the carbon through the functionalization processes. In comparison, AC-NH_2 shows a more gradual gold uptake in time, accomplishing a complete recovery in 24 h contact time.

3.4.1. Gold adsorption mechanism under acidic conditions

XPS analysis corroborates the presence of gold on the carbon's surface when the adsorption is carried out under acid conditions (pH 4).

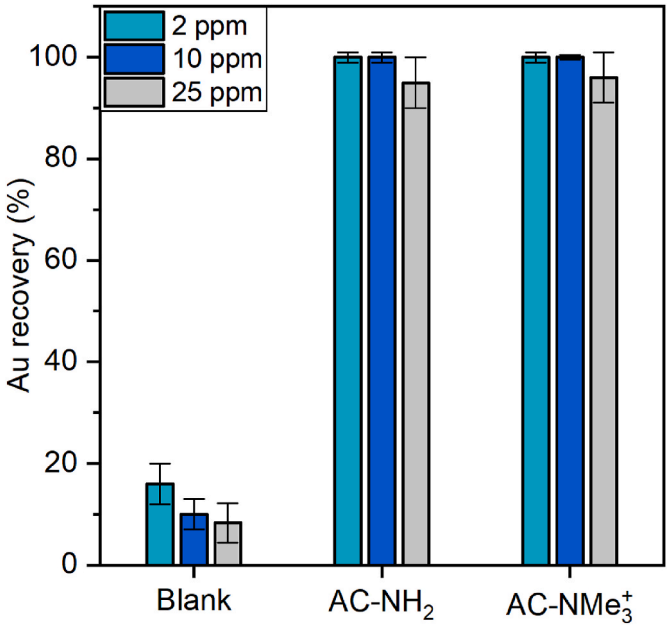

Fig. 7. Non-functionalized (Blank) and aminated (AC-NH_2, AC-NMe_3^+) active carbons gold recovery performances at different gold thiosulfate initial concentrations (Adsorption tests carried out at pH 4). (For interpretation of the references to colour in this figure legend, the reader is referred to the Web version of this article.)

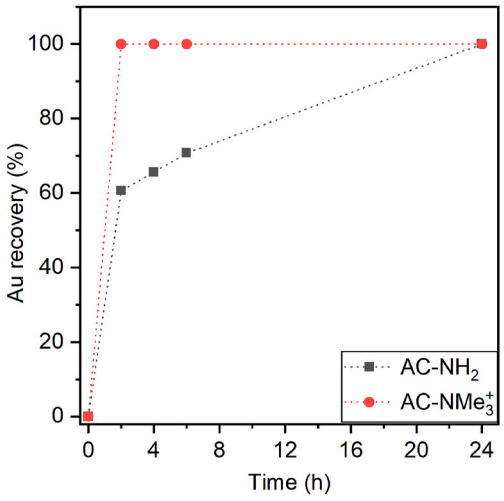

Fig. 8. AC-NH_2 and AC-NMe_3^+ gold adsorption kinetics. Conditions: 25 ppm, 100 mL, pH 4. (For interpretation of the references to colour in this figure legend, the reader is referred to the Web version of this article.)

Firstly, when analyzing AC-NH_2.Au.pH4 (Fig. S2 A) with a high resolution window centered at ≈ 87 eV, the typical Au 4f doublet (Au $4f_{7/2}$ and Au $4f_{5/2}$) is evidenced. Its Au 4 $f_{7/2}$ component is located at ≈ 84.7 eV, which indicates the existence of gold species on the carbon's surface, in which the metal is in oxidation state +1 [55], since the position of pure Au° is expected to appear at lower binding energies (≈83.95 eV) [56,57]. A similar peak is found in the Au 4f HR window of AC-NMe_3^+.AupH4 (Fig. S 2 B), whose Au $4f_{7/2}$ component is positioned at 84.6 eV, revealing as well the presence of Au^{1+} species. Then, when comparing the XPS peaks' positions of the N 1s components (Table 2) before (samples: AC-NH_2 and AC-NMe_3^+) and after (samples: AC-NH_2.Au.pH4 and AC-NMe_3^+.Au.pH4) gold loading, it is noticed that there is not a significant shift in the position of any of the N species after contacting the gold solution. This suggests that no covalent interaction has occurred between $[Au(S_2O_3)_2]^{3-}$and amine sites, since it has been reported in the literature [58] that when amine groups form a covalent bonding with Au, the nitrogen peak (assigned to amines: N-(C,H)) is expected to shift towards lower binding energies (396.6–398.1.eV), like what happens when Au nitride (Au_xN) structures are formed, for example. This information is confirmed by TOF-SIMS analysis of AC-NH_2.Au.pH4 and AC-NMe_3^+.AupH4, since no Au_xN fragments were detected.

Instead, in this case, the adsorption of gold thiosulfate on the aminated carbons at pH 4 may occur mainly due to electrostatic interactions, between the protonated amine groups and $[Au(S_2O_3)_2]^{3-}$, like what occurs with basic resins presenting amine sites [6]. Indeed, as shown in Fig. S 3, the Au–S^- ($m/z \approx 228.95$) fragment and even Au–$S_2O_3^-$ fragment ($m/z \approx 308.93$) were detected by TOF-SIMS in the negative mode in both aminated samples, which verifies this hypothesis. Additionally, a reduction of the normalized intensity of the peak $F_3{}^{34}CSO_2O^-$ ($m/z \approx 151.0$) in the AC-NMe_3^+.Au.pH4 sample is observed, compared to the normalized intensity of the same peak in AC-NMe_3^+, corroborating that this counter-ion is interchanging with Au thiosulfate, when the latter is interacting with the quaternary amine site (Fig. 9).

Lastly, in Table 2, when comparing the total nitrogen surface content detected by XPS (at.%, excluding H) of aminated (AC-NH_2, AC-NMe_3^+) and gold loaded samples (AC-NH_2.Au.pH4, AC-NMe_3^+. Au.pH4), it could be evidenced that the amount of N quantified by XPS remains almost unchanged after gold adsorption, which verifies that the covalent amine grafting in the carbon is strong, and no nitrogen functions are lost during the adsorption process.

3.4.2. Gold adsorption under basic conditions and PZC interpretation

Since pH is an important factor when considering amines as

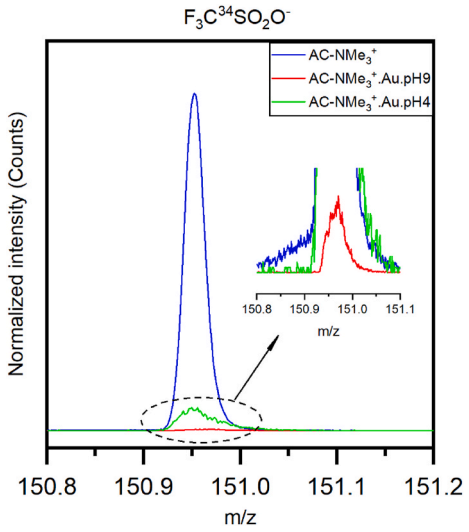

Fig. 9. TOF-SIMS analysis. Comparison between normalized intensities of $F_3{}^{34}CSO_2O^-$ fragment in AC-NMe$_3^+$, AC-NMe$_3^+$.Au pH4 and AC-NMe$_3^+$.Au pH9.

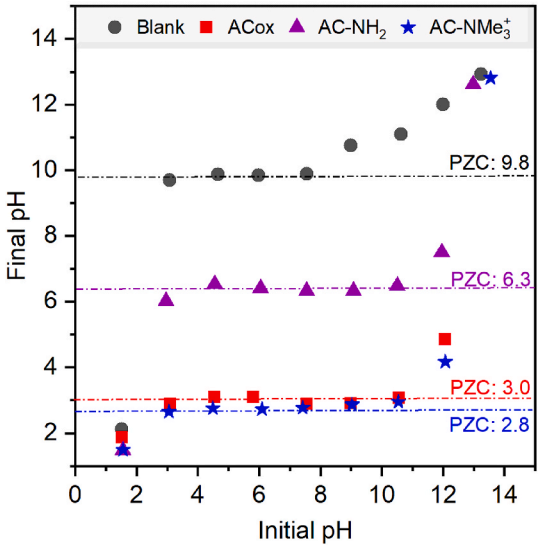

Fig. 10. PZC measurements of non-functionalized (Blank), oxidized (ACox) and aminated samples (AC-NH$_2$, AC-NMe$_3^+$).

functional groups, further research was done to assess the impact on gold adsorption on the aminated carbons, when the adsorption was carried out under acid (pH 4) or basic conditions (pH 9). At this point, it is imperative to differentiate between the influence of pH onto primary and quaternary amine sites. For instance, it is known that primary amines are highly dependent on the solution's pH, since they must be protonated to be able to electrostatically attract negative compounds [7] like $[Au(S_2O_3)_2]^{3-}$. In fact, when the adsorption of gold thiosulfate is done using weak-base resins which contain primary amine sites, it is essential to add an acid prior to gold adsorption, to get the amine protonated [6] and accomplish good gold recoveries from the pregnant solution, whose pH is typically in the range of 9–11. In comparison, quaternary amine sites are by essence positively-charged groups at all pH values, and therefore, their gold thiosulfate adsorption performance is not dependent on the pH of the solution. This is the reason why strong-base resins, which contain quaternary amine sites, are preferred for gold recovery in thiosulfate systems [6].

The PZC value allows to determine the pH at which the net surface charge of the carbon is zero [11]. In other words, the PZC will permit to obtain an "average" view of the carbon's surface charge, which will be influenced by the presence of the different functional groups in the complex carbon structure including: oxygen functional groups, amines, and others. Below the PZC value, the surface will be globally positively charged, while above the PZC value, the net surface charge is negative. This tool may potentially help to predict the pH at which most of the primary amine functional groups are more likely to become protonated. Fig. 10 shows the PZC values measured on our different types of active carbons. Firstly, the PZC value of non-functionalized carbon (9.8) suggests that this carbon may have more basic functions than acidic ones. Then, when the carbon is oxidized with HNO_3 (ACox), the PZC of the sample becomes acidic (3.0), due to the numerous acid oxygen groups, which were indeed evidenced by Boehm titrations. Furthermore, when the sample is functionalized with primary amine sites (AC-NH$_2$), the PZC value is measured at 6.3, which means that, theoretically, if the pH of the solution is below 6.3, most primary amine functional groups are more likely to be protonated. Finally, the PZC value of the quaternary aminated sample (AC-NMe$_3^+$) is 2.8, which may mean that the whole charge of the carbon is dominated by the presence of the remaining oxygen functional groups on the carbon's surface, since the quaternary amine sites are "inert" towards acid-base chemical reactions and therefore, will not influence the pH of the solid [59].

Fig. 11 illustrates the performance of these carbons when working at pH 4 and pH 9. Firstly, it is noticed that the gold adsorption capacity of both aminated carbons is similar and barely impacted when working under basic conditions (accomplishing gold recoveries of ≈80 ± 8 %), which is an expected result when the carbon is enriched with quaternary amine sites. Nevertheless, for primary aminated carbon, theoretically, the gold adsorption performance was expected to decrease under basic conditions, since the amount of primary amine sites that may be protonated is supposed to diminish at pHs higher than 6.3 (however, it is important to remark that at pH 9, some primary amine sites might still be protonated, since the pKa of similar amines like propylamine is 10.6 [60]). Additionally, it is noticed that the non-functionalized carbon increases its gold adsorption performance at basic conditions from ≈8 % (pH 4) to ≈ 20 % (pH 9). To explain this phenomena, complementary PXRD analysis was carried out on the gold loaded samples under these two pH conditions, since previous studies have found that carbon materials have a reductive character due to their electron-rich nature [61,62], and therefore, could potentially reduce Au^{1+} compounds to Au^0 [63]. Furthermore, Fotoohi and Mercier [7] hypothesized about the possible presence of Au^0 nanoparticles in primary amine functionalized silica after Au thiosulfate adsorption, based on the position of their Au 4f XPS peak.

Fig. 12 shows the diffraction spectra of activated carbons that have been loaded with gold at acid and basic conditions. It could be observed

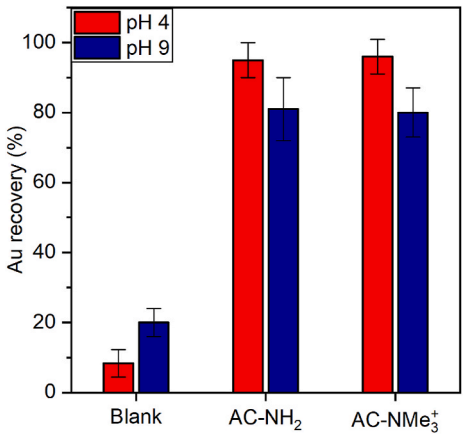

Fig. 11. Influence of pH on gold loading. Gold loading conditions: 25 ppm, 100 ml, 0.5 g AC, pH 4 or pH 9. (For interpretation of the references to colour in this figure legend, the reader is referred to the Web version of this article.)

that when the gold adsorption is carried out under basic conditions, all the samples present several well-defined peaks, whose positions and intensities fit well with the typical Au° reflections found in the Au° simulated spectrum (COD ID 1100138 [64]). Apart from the peaks attributed to Au, three broad humps at 2Θ ≈ 10°, 20° and 34° are also detected, which are assigned to the (002), (100) and (111) reflections of graphite (since active carbons contain small sp^2 organized regions [65]). These broad peaks are observed in all the analyzed samples, including the Blank's (non-functionalized carbon) diffraction spectra. In contrast, when the gold adsorption is carried out at acid pH, no gold reflections are detected in any of the samples. These observations could be explained by the possible formation of Au(OH), which could have been produced due to the abundance of OH^- species under basic conditions. Then, Au(OH) may precipitate on the carbon surface, which will contribute to its reduction to Au° thanks to the electron-rich nature of carbon. Au° is then physically adsorbed on the carbon's surface. This phenomenon could not occur in acidic conditions, where no gold hydroxide could be formed. Additionally, due to aurophilic attraction, it is expected to find Au° nanoparticles on the carbon's surface, since it is known that Au (0) species could bind strongly one to each other in the solid state [62].

XPS analysis of the gold loaded samples under basic conditions gives more information about the type of Au species present in the solid. Firstly, it could be noticed that the Au $4f_{7/2}$ component of the AC-NH_2.Au.pH9 (Fig. S2 C) appears at lower binding energies (84.2 eV) compared to the Au $4f_{7/2}$ peak of the sample at acid conditions (Au $4f_{7/2}$ peak position: 84.7 eV, Fig. S2 A). A similar phenomena is observed in the Au $4f_{7/2}$ peak of the quaternary aminated sample gold-loaded under basic conditions (AC-NMe_3^+.Au.pH9, Fig. S2 D), whose position is 84.3 eV, instead of 84.6 eV (Fig. S 2B). This suggests the presence of new Au species, with a different oxidation state, since the position of these Au peaks is nearer to 83.95 eV (assigned to pure Au°), which is in corroboration with the observations made by PXRD. Interestingly, with TOF-SIMS analysis, the fragments: Au–S ($m/z \approx 228.95$) and AuS_2O_3 ($m/z \approx 308.93$) are detected in both aminated samples (Fig. S 4), which means that $[Au(S_2O_3)_2]^{3-}$ may be present on the carbon, probably acting as counter-ion of positively charged amine groups. Moreover, similarly to what happens in acid conditions with the quaternary amine sample, the $F_3{}^{34}CSO_2O^-$ ($m/z \approx 151.0$) fragment appears in less normalized intensity compared to AC-NMe_3^+, which may mean that this counter-ion is interchanging when $[Au(S_2O_3)_2]^{3-}$ is interacting with the amine site (Fig. 9).

Finally, as shown in Table 2, the Total N content quantified by XPS in the samples loaded under basic conditions remains mostly constant after gold loading, which means that the covalent functions' grafting is not affected under basic conditions (e.g. no functions are lost during gold loading). Additionally, the N 1s components positions do not show any significant shift after gold contact, denoting that the interaction between Au thiosulfate and the charged amine sites may be electrostatic. These results were corroborated by TOF-SIMS analysis done on AC-NH_2. Au. pH9 and AC-NMe_3^+.Au.pH9, where no Au_xN fragments were detected.

Summarizing, when the gold adsorption on primary and quaternary aminated carbons is carried out at basic pHs, various type of Au species are present and therefore, different types of adsorption mechanisms may be taking place at the same time: there are Au (I) thiosulfate species adsorbed as counter-ion of the positively charged primary and quaternary amines sites (as detected by TOF-SIMS), but also some Au° species (evidenced by PXRD and XPS) deposited on the carbon's surface. This is the reason why: 1) primary aminated carbons are performant at adsorbing gold, even at basic pHs, where the amount of protonated amine groups is supposed to decline and 2) Blank enhances its gold recovery when working under basic conditions. In contrast, during the adsorption at acid pHs, no Au° species were evidenced, and therefore, it could be implied that the dominant mechanism in this case may just be ion-exchange interactions. The adsorption mechanisms of aminated carbons under both conditions are illustrated in Fig. 13.

3.5. Elution tests

Once the aminated carbons have been successfully loaded with gold, it is time to consider the elution stage. For this purpose, several eluents that are commonly used for resins' elution [66,67] have been tested. Table 4 shows the elution efficiency of both aminated carbons, whose gold loading stage was carried out under acid or basic conditions.

Regarding the Au loaded carbons under acid conditions, the best elution results are obtained with $Na_2S_2O_3 + NH_4OH$ as eluent, where up to 67 % and 76 % of gold could be stripped off from the primary and quaternary aminated carbons, respectively. The strategy of elution in this case may be accomplished through "Au displacement" in which the adsorption equilibrium between the amine and Au thiosulfate is altered due to the presence of an excess of another anion (in this case, $(S_2O_3)^{2-}$), which would take the place of $[Au(S_2O_3)_2]^{3-}$ as counter-ion, and will return it back in the solution [6], as illustrated in Fig. 14 A. Concerning the stripping with $NaCl + Na_2SO_3$, it is observed that a gold elution of up

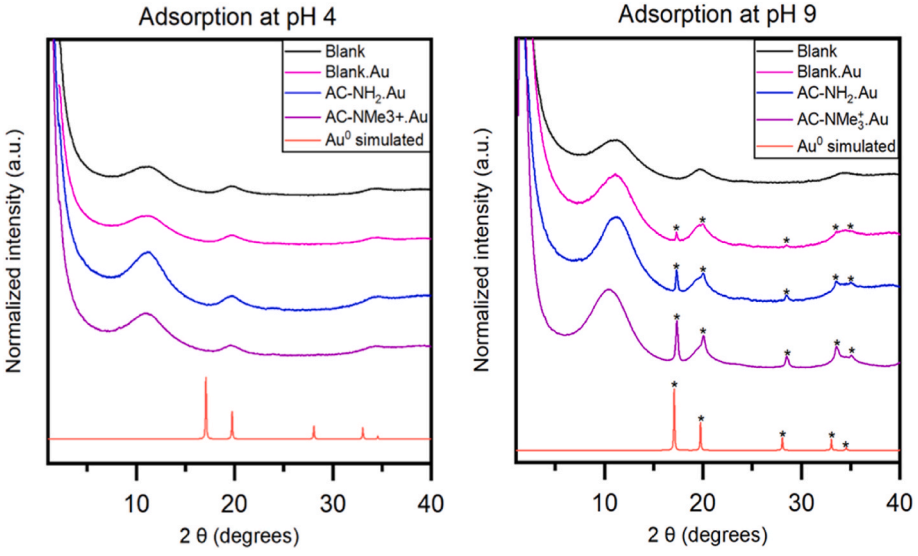

Fig. 12. PXRD analysis of different active carbons loaded with gold under acid and basic conditions. (For interpretation of the references to colour in this figure legend, the reader is referred to the Web version of this article.)

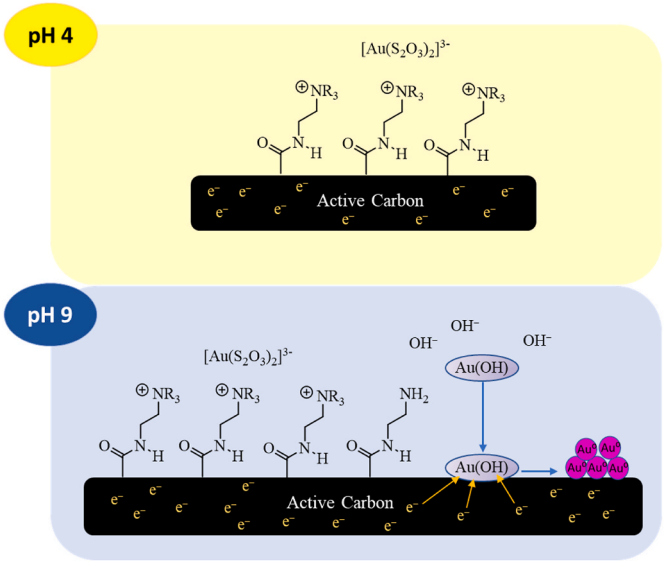

Fig. 13. Scheme representing the possible Au thiosulfate adsorption mechanisms occurring in primary and quaternary amine functionalized carbons when the adsorption is done under acid (pH 4) and basic (pH 9) conditions. R═CH_3 or H.

to 51 % is attained with the primary aminated carbon and 21 % is obtained with the quaternary aminated carbon. In this type of elution, the sulfite anion will first transform $[Au(S_2O_3)_2]^{3-}$ into $[Au(S_2O_3)(SO_3)]^{3-}$ [68], which is known to have a lowest affinity for the amine [6,69]. In fact, Jeffrey et al. [69] and Perera et al. [68], who studied elution strategies of gold thiosulfate in aminated resins, reported that in a system where sulfite species are present, $[Au(S_2O_3)(SO_3)]^{3-}$ is the main complex adsorbed in resins, since it is more stable than $[Au(S_2O_3)_2]^{3-}$ under these conditions. Moreover, they calculated the adsorption equilibrium K values and determined that while $[Au(S_2O_3)_2]^{3-}$ has a K value of 0.53, the mixed complex $[Au(S_2O_3)(SO_3)]^{3-}$ has a K value of 0.0003. Therefore, its affinity for the resin is much lower than $[Au(S_2O_3)_2]^{3-}$. In consequence, $[Au(S_2O_3)(SO_3)]^{3-}$ could be displaced by Cl^-, which is present in high concentration in the eluent [6,69]. This elution strategy is illustrated in Fig. 14 B.

TOF-SIMS and XPS analysis corroborate the successful gold stripping. Indeed, it is noticed that the quantity of Au detected by XPS is notably reduced after elution in all samples, as shown in Table 5. Additionally, the anions $(S_2O_3)^{2-}$ and Cl^- are detected by TOF-SIMS analysis in both eluted samples (Figs. S5 and S6). Some of these anions may be taking part as counter-ions of the charged amine groups and some others may come from eluent residue, still present on the carbon surface.

Furthermore, when the elution is carried out with the samples whose gold loading was done under basic conditions, it could be observed that the elution efficiency decreases with all eluents and types of sample (Table 4). However, an elution of up to 50 % and 56 % is still accomplished for primary and quaternary amine samples, respectively, using $Na_2S_2O_3$ + NH_4OH as eluent. This reduction of efficiency may be due to the presence of Au° in the samples, which would be more difficult to strip than $[Au(S_2O_3)_2]^{3-}$. XPS and TOF-SIMS analysis done on the eluted solids show similar results in the samples gold-loaded at acid conditions: a notable reduction of Au detected by XPS is confirmed (Table 5), and the anions Cl^- and $(S_2O_3)^{2-}$ are detected by TOF-SIMS analysis in both eluted carbons (Figs. S5 and S6), with similar characteristics as stated above.

It is important to highlight that the elution yields that have been accomplished in this research are promising, since the stripping has been carried out under mild conditions and using green eluents. In fact, in the Zadras Elution process that is commonly employed to strip AuCN from loaded activated carbons, the elution solution (typically containing 1% sodium hydroxide and 0.2% sodium cyanide) is recirculated for 72 h at 100 °C to achieve acceptable stripping yields. Working under this kind of conditions causes fine carbon generation, which is lost in mineral tails, along with its bearing gold [32,70]. Therefore, it is imperative to propose alternatives where good elution yields can be obtained, minimizing the mechanical impact of the solid.

4. Conclusions

Granular active carbon has been successfully functionalized with primary and quaternary amine sites through covalent bonds. These functionalized carbons have been tested with gold thiosulfate solution and a remarkable enhancing of gold adsorption performance after treatment has been proven working under acid and basic pHs. Kinetics studies reveal that quaternary aminated carbon is the most efficient one, accomplishing 100 % gold recoveries in 2 h contact time, compared to non-functionalized material that gives < 18% recovery under similar conditions. Regarding primary-aminated AC, a 60% Au recovery is achieved after 2 h of contact, while complete Au recovery is obtained after 24 h. The performances of both functionalized supports are slightly affected by pH conditions, obtaining in all cases a gold adsorption >80 %. The adsorption mechanism taking place in aminated carbons depends on the pH of the gold solution: under acidic conditions, an ion exchange mechanism seems to be the dominant mechanism of gold adsorption. In contrast, under basic conditions, the formation of Au° species has been evidenced, in addition to ion-exchange phenomena. The best gold elution results are accomplished using $Na_2S_2O_3$ and NH_4OH with both aminated carbons, gold loaded at acid and basic conditions (up to 76% for AC-NMe_3^+ and 67% for AC-NH_2). Additionally, NaCl + Na_2SO_3 shows promising elution results, especially in samples which were gold-loaded at acid conditions (up to 21% for AC-NMe_3^+ and 51% for AC-NH_2). Hardness tests show that the functionalized carbons have the desired mechanical properties for being employed in Carbon-in-Pulp processes (H >86 %), without further pelletization, giving these carbons a high competitive advantage compared to strong-base resins.

CRediT authorship contribution statement

Nathalie de la Torre-Miranda: Writing – original draft, Conceptualization, Methodology, Investigation, Formal analysis, Visualization, Writing – review & editing. **Pierre Eloy:** Data curation, Formal analysis.

Table 4
Elution efficiency results with different eluents carried out with samples loaded with Au under acid and basic conditions.

Eluent (molar concentration)	Efficiency (%)			
	Au adsorption at pH 4		Au adsorption at pH 9	
	AC-NH_2	AC-NMe_3^+	AC-NH_2	AC-NMe_3^+
NaCl (2M) + Na_2SO_3 (0,1M)	51 %	21 %	45 %	14 %
$Na_2S_2O_3$ (1M) + NH_4OH (0,14M)	67 %	76 %	50 %	56 %

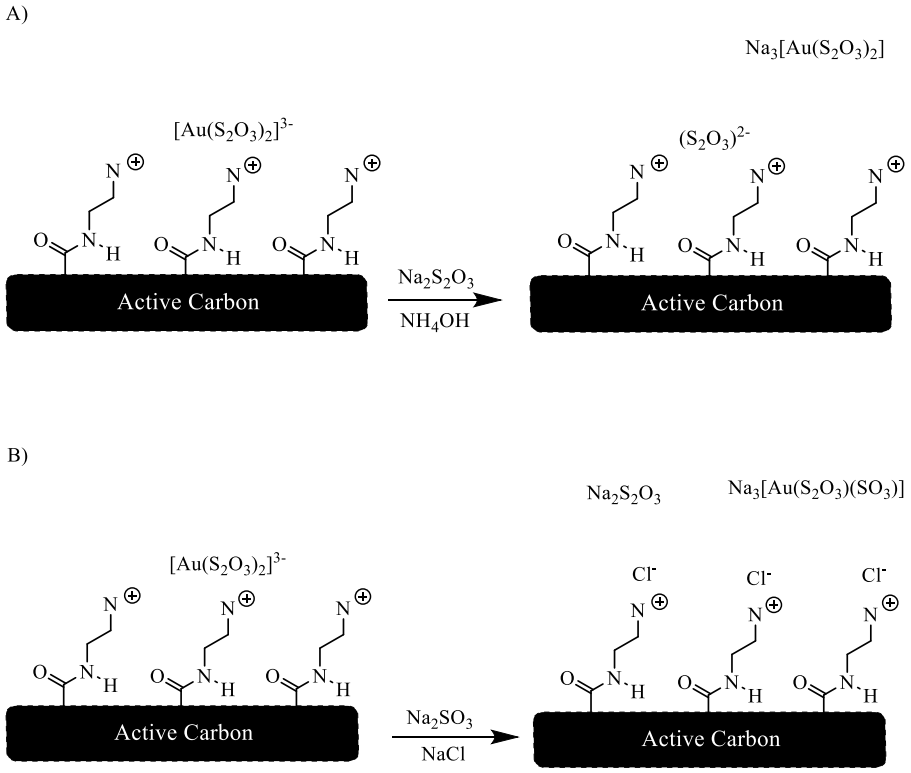

Fig. 14. Scheme illustrating the gold elution strategy using A) $Na_2S_2O_3$ + NH_4OH and B) NaCl + Na_2SO_3 as eluents.

Table 5
Total Au surface content quantified by XPS in gold loaded and eluted samples.

Stage	Eluent	Total Au surface content (at.% excluding H)			
		Au adsorption pH 4		Au adsorption pH 9	
		AC-NH_2	AC-NMe_3^+	AC-NH_2	AC-NMe_3^+
Gold loading	———	0.251	0.275	0.226	0.205
Elution	NaCl + Na_2SO_3	0.015	0.151	0.027	0.170
	$Na_2S_2O_3$ + NH_4OH	0.005	0.001	0.020	0.027

Ernesto de la Torre: Methodology, Investigation, Formal analysis. **Timothy Steenhaut:** Data curation, Formal analysis. **Claude Poleunis:** Data curation, Formal analysis. **Sophie Hermans:** Conceptualization, Supervision, Resources, Project administration, Funding acquisition, Writing – review & editing.

Declaration of competing interest

The authors declare that they have no known competing financial interests or personal relationships that could have appeared to influence the work reported in this paper.

Data availability

Data will be made available on request.

Acknowledgements

The authors are thankful to Conseil d'Action International (CAI) and ARES scholarship programs for funding this research. We thank Jean François Statsyns from UCLouvain and Prof. Alicia Guevara, Mg. Evelyn Criollo and Ing. Kleber Geovany from DEMEX-EPN for their technical support and constant help.

Appendix A. Supplementary data

Supplementary data to this article can be found online at https://doi.org/10.1016/j.matchemphys.2023.128657.

References

[1] B. Xu, W. Kong, Q. Li, Y. Yang, T. Jiang, X. Liu, A review of thiosulfate leaching of gold: focus on thiosulfate consumption and gold recovery from pregnant solution, Metals (Basel) 7 (2017) 1–16, https://doi.org/10.3390/met7060222.
[2] M.G. Aylmore, D.M. Muir, Thiosulfate leaching of gold-a review, Miner. Eng. 14 (2001) 135–174, https://doi.org/10.1016/S0892-6875(00)00172-2.
[3] G. Chi, M.C. Fuerstenau, J.O. Marsden, Study of Merrill-Crowe processing. Part I: solubility of zinc in alkaline cyanide solution, Int. J. Miner. Process. 49 (1997) 171–183.
[4] W.P. Staunton, Carbon-in-Pulp, Gold Ore Process (2016) 535–552, https://doi.org/10.1016/B978-0-444-63658-4.00030-X.
[5] C. Abbruzzese, P. Fornari, R. Massidda, F. Vegliò, S. Ubaldini, Thiosulphate leaching for gold hydrometallurgy, Hydrometallurgy 39 (1995) 265–276, https://doi.org/10.1016/0304-386X(95)00035-F.
[6] Z. Dong, T. Jiang, B. Xu, Y. Yang, Q. Li, Recovery of gold from pregnant thiosulfate solutions by the resin adsorption technique, Metals (Basel) 7 (2017) 95–111, https://doi.org/10.3390/met7120555.
[7] B. Fotoohi, L. Mercier, Some insights into the chemistry of gold adsorption by thiol and amine functionalized mesoporous silica in simulated thiosulfate system,

Hydrometallurgy 156 (2015) 28–39, https://doi.org/10.1016/j.hydromet.2015.05.010.
[8] S.R. La Brooy, H.G. Linge, G.S. Walker, Review of gold extraction from ores, Miner. Eng. 7 (1994) 1213–1241, https://doi.org/10.1016/0892-6875(94)90114-7.
[9] Deborah Chung, Carbon materials, in: Science and Applications, vol. 3, Engineering Materials for Technological Needs, New York, 2019.
[10] C.Y. Yin, M.K. Aroua, W.M.A.W. Daud, Review of modifications of activated carbon for enhancing contaminant uptakes from aqueous solutions, Sep. Purif. Technol. 52 (2007) 403–415, https://doi.org/10.1016/j.seppur.2006.06.009.
[11] P. Chingombe, B. Saha, R.J. Wakeman, Surface modification and characterisation of a coal-based activated carbon, Carbon N. Y. 43 (2005) 3132–3143, https://doi.org/10.1016/j.carbon.2005.06.021.
[12] B. Roop, G. Meenakshi, Activated Carbon Adsorption, Ilustrada, CRC Press, 2005.
[13] W. Shen, W. Fan, Nitrogen-containing porous carbons: synthesis and application, J. Mater. Chem. A 1 (2013) 999–1013, https://doi.org/10.1039/c2ta00028h.
[14] J.Y. Yook, J. Jun, S. Kwak, Amino functionalization of carbon nanotube surfaces with NH 3 plasma treatment, Appl. Surf. Sci. 256 (2010) 6941–6944, https://doi.org/10.1016/j.apsusc.2010.04.075.
[15] B. Ruelle, S. Peeterbroeck, R. Gouttebaron, T. Godfroid, F. Monteverde, J. P. Dauchot, M. Alexandre, M. Hecq, P. Dubois, Functionalization of carbon nanotubes by atomic nitrogen formed in a microwave plasma Ar + N2 and subsequent poly(ε-caprolactone) grafting, J. Mater. Chem. 17 (2007) 157–159, https://doi.org/10.1039/b613581c.
[16] B. Khare, P. Wilhite, B. Tran, E. Teixeira, K. Fresquez, D.N. Mvondo, C. Bauschlicher, M. Meyyappan, Functionalization of carbon nanotubes via nitrogen glow discharge, J. Phys. Chem. B 109 (2005) 23466–23472, https://doi.org/10.1021/jp0537254.
[17] A. Alam, C. Wan, T. McNally, Surface amination of carbon nanoparticles for modification of epoxy resins: plasma-treatment vs. wet-chemistry approach, Eur. Polym. J. 87 (2017) 422–448, https://doi.org/10.1016/j.eurpolymj.2016.10.004.
[18] G. Yang, Y. Li, R.K. Rana, J.J. Zhu, Pt-Au/nitrogen-doped graphene nanocomposites for enhanced electrochemical activities, J. Mater. Chem. A 1 (2013) 1754–1762, https://doi.org/10.1039/c2ta00776b.
[19] A. Bagreev, J.A. Menendez, I. Dukhno, Y. Tarasenko, T.J. Bandosz, Bituminous coal-based activated carbons modified with nitrogen as adsorbents of hydrogen sulfide, Carbon N. Y. 42 (2004) 469–476, https://doi.org/10.1016/j.carbon.2003.10.042.
[20] W. Chouyyok, Y. Shin, J. Davidson, W. Samuels, L. Nikki, R. Rutledge, G. Fryxell, T. Sangvanich, Y. Wassana, Selective removal of copper (II) from natural aters by nanoporous sorbents functionalized with chelating diamines, Environ. Sci. Technol. 44 (2010) 6390–6395, https://doi.org/10.1021/es101165c.
[21] C. De Stefano, O. Giuffrè, S. Sammartano, Protonation constants of ethylenediamine, diethylenetriamine, and spermine in NaCl(aq), NaI(aq), (CH3) 4NCl(aq), and (C 2H5)4NI(aq) at different ionic strengths and t = 25 °C, J. Chem. Eng. Data 50 (2005) 1917–1923, https://doi.org/10.1021/je050177e.
[22] L. Zhao, X. Hu, F. Zi, S. Chen, H. Cheng, P. Yang, Y. Zhang, Y. Chen, Y. Jiang, X. Li, Y. Lin, Z. Li, J. Li, H. Wang, Y. Li, Development of stable, efficient, and recyclable amine-containing microspheres for gold(I) thiosulfate complex recovery, ACS Sustain. Chem. Eng. 10 (2022) 14624–14635, https://doi.org/10.1021/acssuschemeng.2c05267.
[23] D. Vidick, A.F. Leonard, C. Poleunis, A. Delcorte, M. Devillers, S. Hermans, Phosphine- and ammonium-functionalized ordered mesoporous carbons as supports for cluster-derived metal nanoparticles, Catal. Today 235 (2014) 112–126, https://doi.org/10.1016/j.cattod.2014.03.017.
[24] D. Vidick, M. Herlitschke, C. Poleunis, A. Delcorte, R. Hermann, M. Devillers, S. Hermans, Comparison of functionalized carbon nanofibers and multi-walled carbon nanotubes as supports for Fe-Co nanoparticles, J. Mater. Chem. A 1 (2013) 2050–2063, https://doi.org/10.1039/c2ta00131d.
[25] C. Willocq, S. Hermans, M. Devillers, Active carbon functionalized with chelating phosphine groups for the grafting of model Ru and Pd coordination compounds, J. Phys. Chem. 112 (2008) 5533–5541, https://doi.org/10.1021/jp076799j.
[26] J.R. Park, Jaehyeon, Ragabulto, A simple, accurate determintion of oxide PZC and the strong buffering effect of the oxide surfaces at incipient wetness, J. Colloid Interface Sci. 175 (1995) 239–252.
[27] H.P. Boehm, Chemical identification of surface groups, Adv. Catal. 16 (1966) 179–274, https://doi.org/10.1016/S0360-0564(08)60354-5.
[28] A.C. Tarasuk, H.A. Andreas, A.M. Oickle, S.L. Goertzen, K.D. Thériault, Standardization of the Boehm titration. Part I. CO2 expulsion and endpoint determination, Carbon N. Y. 48 (2009) 1252–1261, https://doi.org/10.1016/j.carbon.2009.11.050.
[29] Y.O. Abdalla, A.M. Oickle, H.A. Andreas, K.R. Hopper, S.L. Goertzen, Standardization of the Boehm titration: Part II. Method of agitation, effect of filtering and dilute titrant, Carbon N. Y. 48 (2010) 3313–3322, https://doi.org/10.1016/j.carbon.2010.05.004.
[30] ASTM, ASTM Standard D3802-79, Stand. Test Method Ball-Pan Hardness Act. Carbon, 1999, p. 3, https://doi.org/10.1520/D3802-79R99, 2017.
[31] P.C. Velásquez-López, M.M. Veiga, B. Klein, J.A. Shandro, K. Hall, Cyanidation of mercury-rich tailings in artisanal and small-scale gold mining: identifying strategies to manage environmental risks in Southern Ecuador, J. Clean. Prod. 19 (2011) 1125–1133, https://doi.org/10.1016/j.jclepro.2010.09.008.
[32] W. Stange, The process design of gold leaching and carbon-in-pulp circuits, J. South African Inst. Min. Metall. January/Farmaco (1999) 13–26.
[33] R.B. Cevallos Toledo, C.F. Aragón-Tobar, S. Gámez, E. de la Torre, Reactivation process of activated carbons: effect on the mechanical and adsorptive properties, Molecules 25 (2020) 1–18, https://doi.org/10.3390/molecules25071681.
[34] S.S. Barton, M.J.B. Evans, E. Halliop, J.A.F. MacDonald, Acidic and basic sites on the surface of porous carbon, Carbon N. Y. 35 (1997) 1361–1366, https://doi.org/10.1016/S0008-6223(97)00080-8.
[35] C. Moreno-Castilla, M.A. Ferro-García, J.P. Joly, I. Bautista-Toledo, F. Carrasco-Marín, J. Rivera-Utrilla, Activated carbon surface modifications by nitric acid, hydrogen peroxide, and ammonium peroxydisulfate treatmenss, Langmuir 11 (1995) 4386–4392, https://doi.org/10.1021/la00011a035.
[36] H.P. Boehm, Surface oxides on carbon and their analysis: a critical assessment, Carbon N. Y. 40 (2002) 145–149, https://doi.org/10.1016/S0008-6223(01)00165-8.
[37] N. Karousis, N. Tagmatarchis, D. Tasis, Current progress on the chemical modification of carbon nanotubes, Chem. Rev. 110 (2010) 5366–5397, https://doi.org/10.1021/cr100018g.
[38] S. Hermans, C. Diverchy, O. Demoulin, V. Dubois, E.M. Gaigneaux, M. Devillers, Nanostructured Pd/C catalysts prepared by grafting of model carboxylate complexes onto functionalized carbon, J. Catal. 243 (2006) 239–251, https://doi.org/10.1016/j.jcat.2006.07.019.
[39] S. Shin, J. Jang, S.H. Yoon, I. Mochida, A study on the effect of heat treatment on functional groups of pitch based activated carbon fiber using FTIR, Carbon N. Y. 35 (1997) 1739–1743, https://doi.org/10.1016/S0008-6223(97)00132-2.
[40] G. Socrates, Infrared and Raman Characteristic Group Frequencies, third ed., John Wiley & Sons Ltd., England, 2001.
[41] S. Aduru, S. Contarini, J.W. Rabalais, Electron-, X-ray-, and ion-stimulated decomposition, J. Phys. Chem. 90 (1986) 1683–1688.
[42] B. Stöhr, H.P. Boehm, R. Schlögl, Enhancement of the catalytic activity of activated carbons in oxidation reactions by thermal treatment with ammonia or hydrogen cyanide and observation of a superoxide species as a possible intermediate, Carbon N. Y. 29 (1991) 707–720, https://doi.org/10.1016/0008-6223(91)90006-5.
[43] S.R. Kelemen, M. Afeworki, M.L. Gorbaty, P.J. Kwiatek, M.S. Solum, J.Z. Hu, R. J. Pugmire, XPS and 15N NMR study of nitrogen forms in carbonaceous solids, Energy Fuel. 16 (2002) 1507–1515, https://doi.org/10.1021/ef0200828.
[44] P. Gobbo, M.C. Biesinger, M.S. Workentin, Facile synthesis of gold nanoparticle (AuNP)–carbon nanotube (CNT) hybrids through an interfacial Michael addition reaction, Chem. Commun. 49 (2013) 2831–2833, https://doi.org/10.1039/c3cc00050h.
[45] J.S. Stevens, S.J. Byard, C.A. Muryn, S.L.M. Schroeder, Identification of protonation state by XPS, solid-state NMR, and DFT: characterization of the nature of a new theophylline complex by experimental and computational methods, J. Phys. Chem. B 114 (2010) 13961–13969, https://doi.org/10.1021/jp106465u.
[46] N. Tabet, M. Faiz, A. Al-Oteibi, XPS study of nitrogen-implanted ZnO thin films obtained by DC-Magnetron reactive plasma, J. Electron. Spectrosc. Relat. Phenom. 163 (2008) 15–18, https://doi.org/10.1016/j.elspec.2007.11.003.
[47] A. Amiri, H.Z. Zardini, M. Shanbedi, M. Maghrebi, M. Baniadam, B. Tolueinia, Efficient method for functionalization of carbon nanotubes by lysine and improved antimicrobial activity and water-dispersion, Mater. Lett. 72 (2012) 153–156, https://doi.org/10.1016/j.matlet.2011.12.114.
[48] T. Theophanides, Infrared Spectroscopy- Materials Science, Engineering and Technology, InTechOpen, Croatia, 2012.
[49] A. Hou, Y. Shi, Polymerization and surface active properties of water-soluble amphiphilic polysiloxane copolymers modified with quaternary ammonium salts and long-carbon chain groups, Mater. Sci. Eng. B Solid-State Mater. Adv. Technol. 163 (2009) 99–104, https://doi.org/10.1016/j.mseb.2009.05.014.
[50] K. Gao, Y. Guo, Q. Niu, L. Han, L. Zhou, L. Wang, Quaternary ammonium-functionalized carbon dots for sensitive and selective detection of 2,4,6-trinitrophenol in aqueous medium, Sensor. Actuator. B Chem. 262 (2018) 298–305, https://doi.org/10.1016/j.snb.2018.02.008.
[51] Y. Zhang, Y. Zhang, L. Wang, H. Jiang, C. Xiong, Coconut shell activated carbon supported quaternary ammonium for continuous cycloaddition of CO2 and biogas upgrading in a packed bed, Ind. Eng. Chem. Res. 54 (2015) 5894–5900, https://doi.org/10.1021/acs.iecr.5b00331.
[52] F. Adib, A. Bagreev, T.J. Bandosz, Adsorption/oxidation of hydrogen sulfide on nitrogen-containing activated carbons, Langmuir 16 (2000) 1980–1986, https://doi.org/10.1021/la990926o.
[53] M. Yalcin, A.I. Arol, Gold cyanide adsorption characteristics of activated carbon of non-coconut shell origin, Hydrometallurgy 63 (2002) 201–206, https://doi.org/10.1016/S0304-386X(01)00203-1.
[54] W. Faulkner, J. Urbanic, R. Ruckel, Activated carbon for precious metals recovery, in: 110th Anu. Meet., Soc. Min. Eng. Metall. Soc., Denver, 1987.
[55] A. McNeillie, D.H. Brown, W.E. Smith, M. Gibson, L. Watson, X-ray photoelectron spectra of some gold compounds, J. Chem. Soc., Dalton Trans. (1980) 767–770, https://doi.org/10.1039/DT9800000767.
[56] NIST X-ray Photoelectron Spectroscopy Database, NIST Standard Reference Database Number 20, National Institute of Standards and Technology, Gaithersburg MD, 2000, 20899, https://doi.org/10.18434/T4T88K (retrieved [december, 2022]).
[57] G. Greczynski, L. Hultman, The same chemical state of carbon gives rise to two peaks in X-ray photoelectron spectroscopy, Sci. Rep. 11 (2021) 1–5, https://doi.org/10.1038/s41598-021-90780-9.
[58] A. Adenier, M.M. Chehimi, I. Gallardo, J. Pinson, N. Vilà, Electrochemical oxidation of aliphatic amines and their attachment to carbon and metal surfaces, Langmuir 20 (2004) 8243–8253, https://doi.org/10.1021/la049194c.
[59] T. Suhara, H. Fukui, M. Yamaguchi, Fine silica powder modified with quaternary ammonium groups 2. The influence of electrolyte and pH, Colloids Surfaces A Physicochem. Eng. Asp. 101 (1995) 29–37. SSDI:0927-7757(95)03199-5.

[60] Chemicalbook Inc, Chemical book, propylamine. https://www.chemicalbook.com/ChemicalProductProperty_EN_CB8401908.htm, 2006. (Accessed 13 September 2022).
[61] H. Yang, X. Cui, X. Dai, Y. Deng, F. Shi, Carbon-catalysed reductive hydrogen atom transfer reactions, Nat. Commun. 6 (2015) 1–11, https://doi.org/10.1038/ncomms7478.
[62] S. Hermans, A. Deffernez, M. Devillers, Preparation of Au-Pd/C catalysts by adsorption of metallic species in aqueous phase for selective oxidation, Catal. Today 157 (2010) 77–82, https://doi.org/10.1016/j.cattod.2010.04.010.
[63] G. Bond, C. Louis, D. Thompson, Catalysis by Gold, sixth ed., Imperial College Press, London, 2006.
[64] A. Vaitkus, A. Merkys, S. Gražulis, Validation of the crystallography open database using the crystallographic information framework, J. Appl. Crystallogr. 54 (2021), https://doi.org/10.1107/S1600576720016532.
[65] A. Lazzarini, A. Piovano, R. Pellegrini, G. Agostini, S. Rudić, C. Lamberti, E. Groppo, Graphitization of activated carbons: a molecular-level investigation by INS, DRIFT, XRD and Raman techniques, Phys. Procedia 85 (2016) 20–26, https://doi.org/10.1016/j.phpro.2016.11.076.
[66] H. Arima, T. Fujita, W.T. Yen, Gold recovery from Nickel catalyzed ammonium thiosulfate solution by strongly basic anion exchange resin, Mater. Trans. 44 (2003) 2099–2107, https://doi.org/10.2320/matertrans.44.2099.
[67] S. Gámez, K. Garcés, E. de la Torre, A. Guevara, Precious metals recovery from waste printed circuit boards using thiosulfate leaching and ion exchange resin, Hydrometallurgy 186 (2019) 1–11, https://doi.org/10.1016/j.hydromet.2019.03.004.
[68] W.N. Perera, G. Senanayake, M.J. Nicol, Interaction of gold(I) with thiosulfate-sulfite mixed ligand systems, Inorg. Chim. Acta. 358 (2005) 2183–2190, https://doi.org/10.1016/j.ica.2004.09.058.
[69] M.I. Jeffrey, D.M. Hewitt, X. Dai, S.D. Brunt, Ion exchange adsorption and elution for recovering gold thiosulfate from leach solutions, Hydrometallurgy 100 (2010) 136–143, https://doi.org/10.1016/j.hydromet.2009.11.003.
[70] M. Soleimani, T. Kaghazchi, Gold recovery from loaded activated carbon using different solvents, J. Chin. Inst. Chem. Eng. 39 (2008) 9–11, https://doi.org/10.1016/j.jcice.2007.11.004.